ELSEVIER

International Journal of Psychophysiology 24 (1996) 189–195

INTERNATIONAL JOURNAL OF PSYCHOPHYSIOLOGY

Application of dimension estimation and surrogate data to the time evolution of EEG topographic variables

Walter S. Pritchard [a,*], Kelly K. Krieble [b,1], Dennis W. Duke [b,c]

[a] *Psychophysiology Laboratory Bowman Gray Technical Center, 611-12, R.J. Reynolds Tobacco Company, Winston-Salem, NC 27102, USA*
[b] *Supercomputer Computations Research Institute, Florida State University, Tallahassee, FL 32306, USA*
[c] *Department of Physics, Florida State University, Tallahassee, FL 32306, USA*

Received 18 December 1995; accepted 13 August 1996

Abstract

Dimensional complexity (estimated correlation dimension) was measured for two topographic EEG time series: (a) the time evolution of global field power (GFP) and (b) the time evolution of sequential dissimilarity (SQD) for resting, eyes-closed and eyes-open data. Eyes-closed GFP and eyes-closed/open SQD all had an element of nonlinearity in their dynamics as evidenced by increased dimensional complexity associated with the phase-angle randomization, Gaussian surrogate-data procedure. However, none of the three gave any evidence of being deterministic chaotic processes. Eyes-open GFP dimensional complexity could not be distinguished from a linear-stochastic process.

Keywords: EEG; Topography; Global field power; Sequential dissimilarity; Correlation dimension; Nonlinear dynamics; Chaos

1. Introduction

This manuscript is part of a series investigating the nonlinear dynamical properties of the human EEG. In the first [[1], see also [2]], the technique of dimension estimation was applied to a set of resting, eyes open and eyes-closed EEG recorded from normal young subjects. Dimension estimation provides a measure (estimated correlation dimension) of the complexity of a system's dynamics reconstructed in state space by the Takens method of delays. When used as a relative EEG measure comparing groups or effects of interest, the dynamically more neutral term *dimensional complexity* is preferred.

In [1], a property termed *saturation* (a leveling off of dimensional complexity with an increase in the dimension of the state space in which the time series is embedded) was found to be good at certain sites on the scalp (data were recorded from the nineteen 10-20 loci). This was interpreted as indicating that the EEG at these loci was produced by low-dimensional, deterministic chaos of the strange-attractor type (in the rest of the manuscript, addition of the phrase 'of the strange-attractor type' to the word 'chaos' will be understood).

The second manuscript [3] was motivated by further developments in the application of nonlinear dynamics to time series data. Specifically, it was shown that 1/f-like, linearly correlated ('colored') noise will 'fool' dimension estimation algorithms in that good saturation is obtained from what is in fact a stochastic system. Thus, good saturation, although

* Corresponding author.
[1] Arkansas School for Math and Sciences, 200 Whittington Avenue, Hot Springs, AK 71901, USA

PII S0167-8760(96)00059-1

a necessary condition for inferring low-dimensional chaos, is not a sufficient condition. The demonstration of deterministic chaos and/or nonlinearity (either deterministic or stochastic) requires an additional procedure termed *surrogate-data testing*.

In surrogate-data testing, dimension estimation is applied to the original time series. The series is then fast Fourier transformed ('FFTed'), the phase angles are randomized, and the data reversed FFTed. The result is a time series having the same power spectrum as the original, but from which nonlinearity has been removed – the surrogate series is linear noise regardless of the nature of the original series. Dimension estimation is then applied to the surrogate series. If the original series was in fact a linear noise, then there is no change in the results of the dimensional analysis. If the original series was nonlinear, then there is an increase in estimated dimension. Finally, if the original series was low-dimensional chaos, then there is both an increase in dimension estimates along with good saturation of the original data.

Using surrogate-data testing, we found that the EEG data originally analyzed in [1] had a significant element of nonlinearity, but did not represent low-dimensional chaos. This finding was subsequently replicated in a different group of subjects [4]. These findings do not mean that our EEG data were stochastic in the strong sense of the word (approaching infinite dimension), but rather that the dimension of our data was at least higher than the ability of dimension estimation to resolve given the limited size of our EEG segments (which consisted of 8 s digitized at 128 Hz for a total of 1024 data points).

In this manuscript, we apply dimension estimation to EEG *topography*. Although on a locus by locus basis, individual EEG time series were nonlinear but not chaotic [3,4], we sought to examine the possibility that emergent chaotic dynamics govern the time evolution of EEG topography. Alternatively, it may be the case that emergent stochastic linearity governs the time evolution of EEG topography even if the dynamics of individual channels is nonlinear. Dimensional complexity was computed for two topographic time series: (a) the time evolution of global field power (GFP) and (b) the time evolution of sequential dissimilarity (SQD).

1.1. Global field power (GFP)

GFP is a measure, at a given instant in time, of the 'hilliness' of the EEG across the scalp, that is, the momentary electric strength of the mapped EEG 'landscape' [5]. It represents the spatial root mean square of all local voltages measured relative to the average reference (and thus is independent of the actual reference employed during recording). Consider a set of M_i EEG channels each consisting of N_j data points. The voltage V of channel i measured at point j is actually the difference in electrical potential between the 'active' electrode on the scalp and the 'reference' electrode (in our case, on the tip of the nose):

$$\delta V_{i,j} = V_{i,j} - V_{reference,j}$$

The average reference transformation $A_{i,j}$ is computed as follows:

$$A_{i,j} = \delta V_{i,j} - [1/N] \sum_{i=1}^{N} \delta V_{i,j}$$

The average reference produces a rejection of the time-varying offset (spatial DC component) measured between the (arbitrarily chosen) recording reference and the 'active' electrode loci on the scalp [5]. This results in a 'virtual' reference that exists, in essence, 'everywhere' in space. Once the data have been transformed to the average reference (M transformed to A), GFP is computed as

$$\left[(1/N) \sum_{n=1}^{N} A_n\right]^{1/2}$$

1.2. Sequential dissimilarity (SQD)

SQD is the *global dissimilarity* between two temporally successive topographic maps. Global dissimilarity is in turn the GFP of the difference map obtained by subtracting two maps normalized to unity GFP [5]. For average-reference map A, the normalized map is X = A/[GFP(A)]. The global dissimilarity D between X and another normalized map Y is given by

$$\left[(1/N) \sum_{n=1}^{N} (X_n - Y_n\right]^{1/2}$$

Because of the normalization, global dissimilarity does not reflect differences in map amplitude, only differences in map *shape*. It thus provides a measure of 'topographic instability', and is inversely related to the spatial correlation between two maps (see [6], Appendix 1, for evidence). Although times of low instability/high stability (low SQD) are usually associated with times of high GFP, one is not necessarily the inverse of the other (cf. [5], Fig. 3a).

2. Method

The EEG data analyzed were those originally collected by Pritchard [7]. Briefly, resting EEG data were recorded from the 19 loci of the international 10-20 system under two conditions (eyes-closed and eyes-open, fixating), with each set of eyes-closed/open recordings being repeated four times (four blocks). Twelve non-smoking subjects having no history of neurologic or psychiatric disorder participated after giving informed consent (5 females, 7 males; average age 27.75, SD 4.25, range 19–34). Subjects were tested in the morning in a soundproof, electrically shielded room while seated in a comfortable chair. Sn electrodes were attached to the scalp loci, the tip of the nose (reference), and the forehead (ground). On-line high- and low-pass filter settings of 0.3 and 30 Hz (-12 dB/octave) were employed with a sampling rate of 128 Hz. All electrode impedances were < 3 kΩ. For each subject, a continuous, 8-s, 19-channel EEG set judged by visual inspection to be in all channels free of electroocular (EOG) and movement artifacts, and to contain minimal electromyographic (EMG) activity, was available for each eyes-closed/open $\times$ block combination (the first artifact-free 8-s set from 120 total seconds of data).

3. Results

3.1. Global field power (GFP)

3.1.1. Dimensional complexity

For each EEG record, GFP was computed at each time point as outlined in the introduction. This was done using 15 of the 19 recording electrodes (loci Fp1, Fp2, T3, and T4 were omitted because of their association with artifacts). The result was, for each EEG record, a 1024-point GFP time series, from which dimensional complexity was estimated for embedding dimensions 4–16 by 2s using the Takens-Ellner method (see [8], for details). Each GFP time series was also submitted to the Gaussian amplitude-adjusted surrogate-data procedure [9], with dimensional complexity again being estimated for the surrogates (Gaussian surrogates not only test against the null hypothesis of a linear-stochastic process, but also control for a static, nonlinear measurement transformation [2]).

The GFP dimensional complexity data were submitted to a four-way, within-subjects analysis of variance (ANOVA; in all ANOVAs results reported, Greenhouse-Geisser-corrected p-values are employed where appropriate). The four variables were eyes closed/open $\times 4$ blocks of recording $\times$ original/surrogate data $\times$ embedding dimension.

The main effect of eyes closed/open was significant [$F(1,11) = 5.54$, $p = 0.0382$], with GFP dimensional complexity being lower for than eyes-closed condition (3.806) than for the eyes-open condition (4.067). The main effect of original/surrogate data was also significant [$F(1,11) = 7.63$, $p = 0.0185$], with GFP dimensional complexity being signficantly increased by the surrogate-data procedure (from 3.899 to 3.974). Finally, the main effect of embedding dimension was significant [$F(6,66) = 176.45$, $p < 0.0001$], with GFP dimensional complexity increasing with increasing embedding dimension. All

[2] Gaussian surrogates [9] consider the possibility that the 'true' EEG x_t is transformed into the observed EEG v_t by a static nonlinear filter h() [$v_t = h(x_t)$]; the filter is static because v_t depends only on the current value of x_t and not on derivatives or past values]. First, a time series g[t] having an independent, identical Gaussian distribution is formed. This series is then re-ordered so that its ranking agrees with the original EEG time series (if v[t = i] is the n^{th} smallest EEG amplitude, then g[t = i] is the n^{th} smallest Gaussian amplitude). Thus, g[t] is a times series that 'follows' v[t] but has a Gaussian amplitude distribution. The Gaussian series is then Fourier transformed, phase-angle shuffled, and reverse Fourier transformed to form g'[t], a surrogate of the Gaussian series. The final surrogate data set is then formed from the original series v[t] by re-ordering it so that it follows g'[t] in the sense that ranks agree.

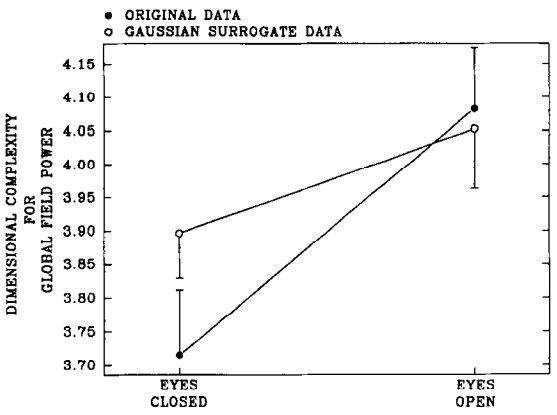

Fig. 1. GFP dimensional complexity: the eyes close/open × original/surrogate two-way interaction. The surrogate-data procedure produced an increase only for the eyes-closed data.

of these main effects were qualified by the interactions presented below.

The interaction of original/surrogate data with eyes closed/open was significant [$F(1,11) = 29.16$, $p = 0.0002$], as illustrated in Fig. 1. As indicated in the figure, the increase in GFP dimensional complexity associated with the surrogate-data procedure was significant only for the eyes-closed condition.

The interaction of original/surrogate data with embedding dimension was also significant [$F(6,66) = 12.65$, $p < 0.0001$]. This interaction is illustrated in Fig. 2, which indicates that the increase in GFP dimensional complexity associated with the surrogate data procedure began at embedding dimension 10 and thereafter increased with increasing embedding dimension. However, this two-way interaction was overshadowed by a significant three-way interaction among eyes closed/open, original/surrogate data, and embedding dimension [$F(6,66) = 11.66$, $p < 0.0001$]. As illustrated in Figs. 3 and 4 (and consistent with Fig. 1), the pattern seen in Fig. 2 was

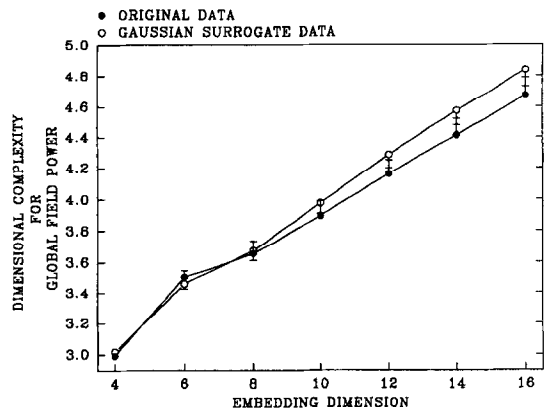

Fig. 2. GFP dimensional complexity: the original/surrogate × embedding dimension interaction. The original versus surrogate difference appears to grow with increasing embedding dimension.

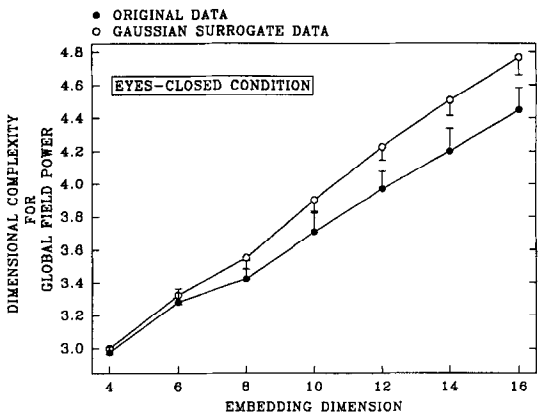

Fig. 3. GFP dimensional complexity, eyes-closed condition: comparing this figure with Figs. 2 and 4 indicates that the pattern seen in Fig. 2 (original versus surrogate difference increasing with increasing embedding dimension) was completely a function of the eyes-closed data. This is consistent with the interaction displayed in Fig. 1.

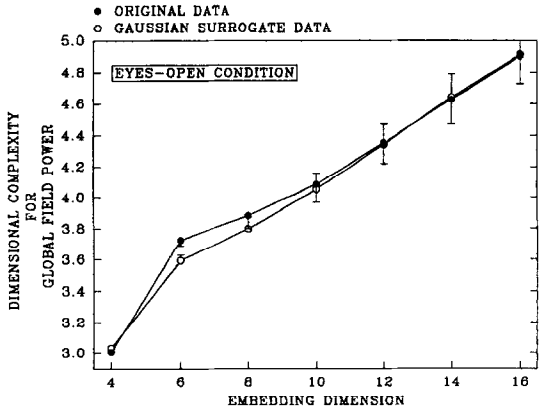

Fig. 4. GFP dimensional complexity, eyes-open condition: comparing this figure with Figs. 2 and 3 indicates that the pattern seen in Fig. 2 (original versus surrogate difference increasing with increasing embedding dimension) was completely a function of the eyes-closed data. This is consistent with the interaction displayed in Fig. 1.

driven entirely by the eyes-closed data – the surrogate data procedure did not systematically affect GFP dimensional complexity in the eyes-open condition.

3.1.2. Saturation slope

Figs. 2–4 indicate no evidence of saturation in the GFP dimensional complexity data – GFP dimensional complexity did not level-off or even begin to level-off with increasing embedding dimension. To assess subtle effects on the saturation properties of GFP dimensional complexity, the slope of dimensional complexity as a function of embedding dimension across dimensions 6–16 was computed for each EEG record as well as its random Gaussian surrogates, with increasingly positive slope indicating increasingly poorer saturation (4 was omitted because the 'jump' from 4 to 8 appeared disproportionate in the eyes-open data). The GFP saturation slope data were submitted to a three-way, within-subjects ANOVA (eyes closed/open × block × original/surrogate data).

The main effect of original/surrogate data was significant [$F(1,11) = 48.58$, $p < 0.001$], with saturation being poorer in the surrogate data (slope = 0.141) than in the original data (slope = 0.120). This main effect was qualified by a significant two-way interaction between eyes closed/open and original/surrogate data [$F(1,11) = 7.88$, $p < 0.0171$]. This interaction is illustrated in Fig. 5, which indicates that the surrogate-data procedure increased GFP saturation slope only in the eyes-closed condition (a pattern that can be seen in Fig. 3). The three-way interaction among eyes closed/open, original/surrogate data, and block was also significant [$F(3,33) = 7.48$, $p = 0.0013$]. This interaction produced no systematically interpretable pattern, and is not illustrated.

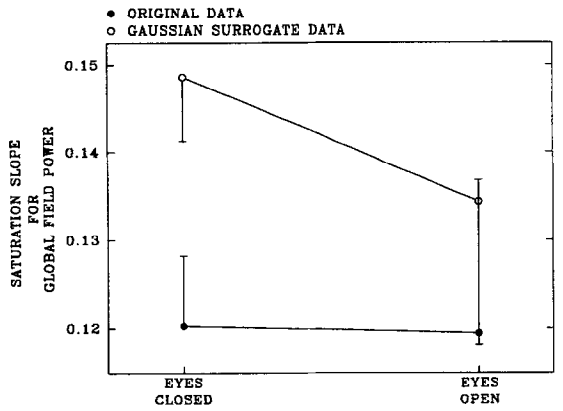

Fig. 5. GFP saturation slope: the eyes close/open × original/surrogate two-way interaction. Consistent with the previous figures, saturation slope was increased by the surrogate-data procedure only in the eyes-closed condition.

3.2. Sequential dissimilarity (SQD)

3.2.1. Dimensional complexity

For each EEG record, SQD was computed at each time point as outlined in the introduction. This was again done using the same 15 loci used for computing GFP. The result was, for each EEG record, a 1023-point SQD time series, from which dimensional complexity was again estimated for embedding dimensions 4–16 by 2s. Each SQD time series was also submitted to the random Gaussian surrogate-data procedure, with dimensional complexity again being estimated for the surrogates. The SQD dimensional complexity data were then submitted to an ANOVA equivalent in design to that used to analyzed GFP dimensional complexity.

The main effect of original/surrogate data was significant [$F(1,11) = 31.92$, $p < 0.0001$], with the surrogate data procedure producing an increase in SQD dimensional complexity from 4.554 to 4.743. The main effect of embedding dimension was also significant [$F(6,66) = 543.15$, $p < 0.0001$], with SQD dimensional complexity increasing with increasing embedding dimension. Both of these main effects were qualified by a significant interaction between original/surrogate data and embedding dimension [$F(6,66) = 11.85$, $p = 0.0005$]. This interaction is illustrated in Fig. 6, which indicates that the surrogate data procedure increased SQD dimensional complexity for all embedding dimensions except 4.

3.2.2. Saturation slope

As for GFP dimensional complexity, there was no apparent saturation in the SQD dimensional complexity (Fig. 6). As was done for GFP dimensional complexity, saturation slope was computed for SQD dimensional complexity, and the results submitted to an ANOVA equivalent in design to that used to analyzed GFP dimensional complexity. No signifi-

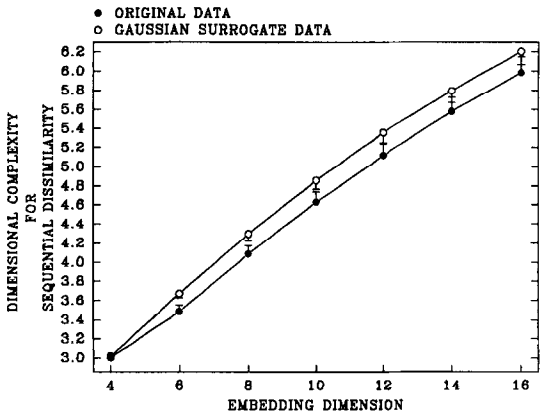

Fig. 6. SQD dimensional complexity: the original/surrogate × embedding dimension interaction. The original versus surrogate difference appears to be constant for embedding dimensions 6 and higher.

cant effects were obtained. As can be seen in Fig. 6, other than the change from embedding dimensions 4 to 6, the slopes for original and surrogate data are virtually identical.

3.3. Relation between GFP dimensional complexity and SQD dimensional complexity

As outlined in the Introduction, times of low SQD are usually associated with times of high GFP, but one is not necessarily the inverse of the other. Similarly, their respective dimensional complexities also appear to be moderately related. For the original data, GFP dimensional complexity was correlated +0.640 with SQD dimensional complexity.

4. Discussion

The time evolution of both ehe eyes-closed 'hilliness' of resting EEG topography (GFP) and eyes-closed and eyes-open sequential changes in the 'shape' of EEG topography (SQD) were all found to have an element of nonlinearity. For all three, surrogate data produced significant increases in dimensional complexity, although the relative magnitude of the increases was not large. In this manner, they resemble the dynamical properties of the same EEG data analyzed as *voltage* time series on a locus by locus basis [3,4]. Thus, they do not represent an 'emergent nonlinear element' only seen when the topographic field is examined. In contrast, the time evolution of eyes-open 'hilliness' could not be distinguished from a linear-stochastic process (there was no evidence of saturation and no change with surrogate data). Thus, the eyes-open GFP time series represents an 'emergent linearity' aspect of the EEG not seen on a locus-by-locus basis.

One may speculate that the nonlinear element of the time evolution of 'hilliness' in the eyes-closed data may be a function of the occipital, eyes-closed alpha rhythm, and that in the absence of the alpha rhythm, resting EEG 'hilliness' evolves as a topographically emergent linear-stochastic process. This notion was born out by a correlation of +0.577 between the increase in GFP dimensional complexity associated with the surrogate-data procedure and average alpha power in each EEG (alpha power latter previously computed in [7]).

There were also differences between eyes-closed GFP and SQD in their nonlinear properties: for eyes-closed GFP, surrogate-data differences appeared to grow with increasing embedding dimension (Fig. 3) – hence the difference in saturation slope between the original data and the surrogate data. In contrast, original/surrogate differences in SQD dimensional complexity were relatively constant across embedding dimensions. The theoretical implications of these differences are unclear, as they have not (to our knowledge) been addressed by theoreticians in the area [9]. We do note that the increase in GFP dimensional complexity with surrogate-data testing was negatively correlated with average locus-by-locus dimensional complexity (−0.400), that is, if the individual-loci EEGs are of low complexity, there tends to be a larger increase in GFP dimensional complexity when the surrogate-data procedure is applied. In contrast, the increase in SQD dimensional complexity with surrogate-data testing was unrelated to locus-by-locus dimensional complexity (correlation of +0.045).

Finally, no evidence of low-dimensional chaos was found for either measure of EEG topography: for both measures under both eyes-closed and eyes-open conditions, dimensional complexity of the original data did show even a trend toward saturating. Thus, the evolution of EEG topographic measures

under testing conditions would appear to be best categorized as stochastic processes, with three of the four having an element of stochastic nonlinearity.

Acknowledgements

The research of DWD and KKK was supported by the US Department of Energy through contract number DE-FC05-85ER250000 as well as by funding from the R.J. Reynolds Tobacco Company.

References

[1] Pritchard, W.S. and Duke, D.W. (1992) Dimensional analysis of no-task human EEG using the Grassberger-Procaccia method. Psychophysiology, 29, 182–192.

[2] Pritchard, W.S., and Duke, D.W. (1990) Deterministic chaos and the human EEG. Psychophysiology, 27, S56.

[3] Pritchard, W.S., Duke, D.W., and Krieble, K.K. (1995) Dimensional analysis of resting human EEG II: Surrogate-data testing indicates nonlinearity but not low-dimensional chaos. Psychophysiology, 27, 486–491.

[4] Pritchard, W.S., Krieble, K.K., and Duke, D.W. (1995) Rapid communication: No Effect of cigarette smoking on electgroencephalographic nonlinearity. Psychopharmacology, 119, 349–351.

[5] Lehmann, D. (1989) From mapping to the analysis and interpretation of EEG/EP maps. In K. Maurer (Ed.), Topographic brain mapping of EEG and evoked potentials, Springer-Verlag, Berlin, pp. 53–75.

[6] Brandeis, D., Naylor, H., Halliday, R., Callaway, E., and Yano, L. (1992) Scopolamine effects on visual information processing, attention, and event-related potential map latencies. Psychophysiology, 29, 315–336.

[7] Pritchard, W.S. (1991) Electroencephalographic effects of cigarette smoking. Psychopharmacology, 104, 485–490.

[8] Pritchard, W.S., and Duke, D.W. (1992) Measuring chaos in the brain: A tutorial review of nonlinear dynamical EEG analysis. Int. J. Neurosci., 67, 31–80.

[9] Theiler, J., Eubank, S., Longtin, A., Galdrikian, B., and Farmer, J.D. (1992) Testing for nonlinearity in time series: The method of surrogate data. Physica D, 58, 77–92.